JACS
JOURNAL OF THE AMERICAN CHEMICAL SOCIETY

COMMUNICATION

pubs.acs.org/JACS

Enhancing Cell Recognition by Scrutinizing Cell Surfaces with a Nanoparticle Array

Hongyu Zhou,[†] Peifu Jiao,[†,‡] Lei Yang,[†] Xi Li,[†] and Bing Yan*[,†,‡]

[†]Department of Chemical Biology and Therapeutics, St. Jude Children's Research Hospital, Memphis, Tennessee 38105, United States
[‡]School of Chemistry and Chemical Engineering, Shandong University, Jinan 250100, China

Supporting Information

ABSTRACT: We report a dual-ligand nanoparticle array approach for discerning cells that have different surface receptor profiles surrounding a common primary receptor expressed at high or low levels. The achieved differentiation provides nanoparticles the ability for potential applications in treatment of patients at a personalized medicine level for drug delivery and radiation therapy with a much better safety profile.

Cell−cell recognition through multivalent interactions between multiple ligand−receptor pairs is an ideal model for nanoparticle cell delivery systems. The current nanoparticle systems achieve cell recognition by functionalization of the nanoparticles with a targeting ligand such as antibodies,[1,2] oligopeptides,[3,4] nucleic acid aptamers,[5−7] carbohydrates,[8−10] or other molecules.[11,12] However, a dilemma is that the single-receptor targeting cannot differentiate cells that happen to have a common receptor, such as cells from different patients with the same disease. Another serious problem is that a receptor overexpressed in diseased cells (e.g., cancer cells) is also expressed at a lower level in normal cells, so a single-ligand targeting system may have off-target effects on normal cells.[13,14] Since cells express multiple surface receptors, the dual-targeting approach has been considered an improvement for cell recognition. Although results from the proof-of-concept experiments with two known receptor ligands have been evaluated,[15−19] this approach is severely hindered in general by the lack of receptor information on the cell surface. Here we address these critical issues by the development of highly selective nanoparticles decorated with dual-targeting molecules through scanning of the cell surface with a dual-ligand nanoparticle array (DLNA) that varies the molecular diversity of the secondary ligands surrounding the primary ligand on gold nanoparticles (GNPs). We demonstrate below that this DLNA can discern the slightest difference between cells that have different surface receptor profiles surrounding a common primary receptor expressed at high or low levels.

Cervical cancer cells (Hela), epidermal cancer cells (KB), and hepatocellular carcinoma cells (HepG2) all overexpress folate receptors (FRs). However, their surface receptor profiles surrounding FRs are likely to be different because of their different origins. We hypothesized that ligands that interact with the secondary receptors surrounding FRs for these cell lines would enhance cell recognition and, more importantly, differentiate these similar cells having a common receptor such as FRs. To test this hypothesis, a DLNA containing 30 members was synthesized. To achieve the maximum surface structural diversity in this DLNA, we selected highly diverse building blocks, including five acylators and six amines. Every folic acid (FA) ligand in this array was surrounded by secondary ligands, which contained diverse molecular structures from combinatorial library synthesis (Figure 1a; detailed information on the synthesis of the second ligand library, thioctic-FA, and DLNA is included in the Supporting Information). Our previous works have shown that combinatorial chemistry modifications on surfaces of nanoparticles altered their interactions with proteins and cells.[20,21] Members of the array were characterized by transmission electron microscopy (TEM; Figure S1 in the Supporting Information), UV−vis spectrometry (Figure S2), dynamic light scattering (DLS; Figure S3), and ζ potential measurements (Table S1 in the Supporting Information). The ratio of the secondary ligand to FA was between 7 and 12 (Table S2), as determined by iodine cleavage and a quantitative HPLC/MS/UV/chemiluminescent nitrogen detection (CLND) method (Figure S4).[22] After integrity confirmation, we examined their cell recognition capabilities by inductively coupled plasma mass spectroscopy (ICP-MS) quantification of GNPs bound to or taken up by cells.

Alternating secondary ligands surrounding FA resulted in different cell recognition patterns, as shown by cell binding and uptake of GNPs (Figure 1b−d and Figures S5−S7). The cell binding and uptake of dual-ligand GNPs was expressed by the relative amounts of cellular gold in comparison with that from binding of monoligand (FA) GNPs (**GNP-FA**; Figure 1b−d). From the heat maps in Figure 1b−d, **D55** and **D56** exhibited cell recognition enhancement by a factor of 3−4 for Hela cells, while **D16** and **D21** exhibited the highest enhancement effects for HepG2 cells. Diverse secondary ligands on dual-ligand GNPs generated different cell recognition patterns, suggesting that the microenvironmental receptor profiles surrounding FRs in these cells are indeed different and that the DLNA approach is highly effective in identifying selective ligands when the cell receptor profile is unknown.

Comparison of the cell recognition of the dual-ligand GNPs with that of each of the monoligand GNPs (**M** is used to indicate GNPs with only the secondary ligand) revealed a 3−10-fold increase of cell binding and uptake for all cells was observed (Figure 2a,b). This enhancement was much more than an

Received: September 21, 2010
Published: December 23, 2010

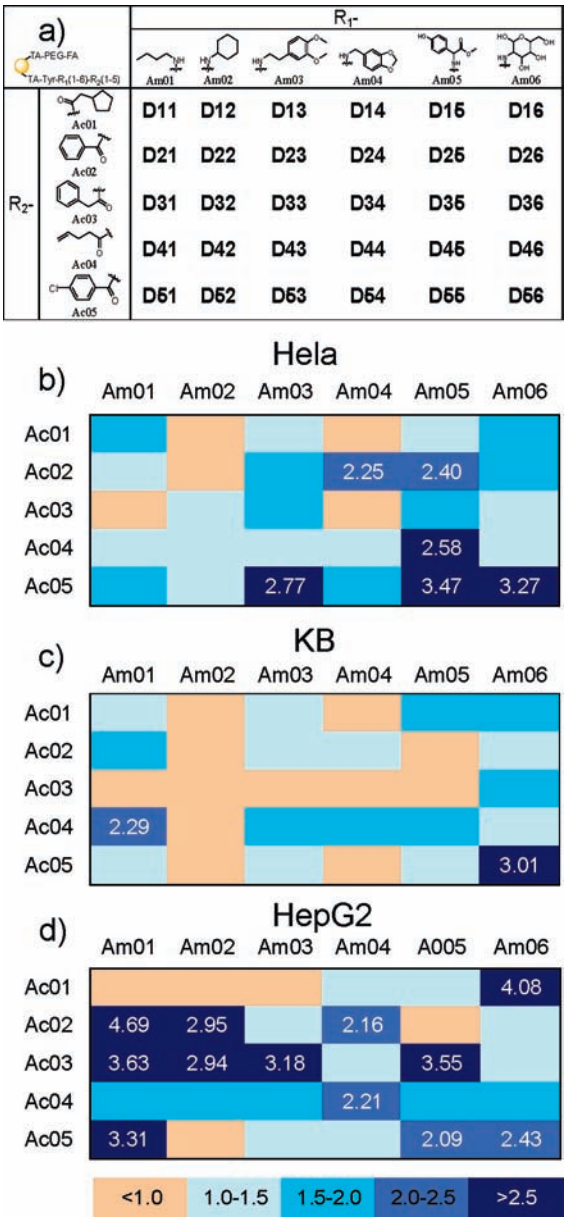

Figure 1. (a) Surface molecular compositions of dual-ligand GNP array members. (b–d) Heat maps showing the relative cellular uptake amounts of dual-ligand GNPs for (b) Hela, (c) KB, and (d) HepG2 cells in comparison with **GNP-FA**. The GNP concentration for all experiments was 50 μg/mL.

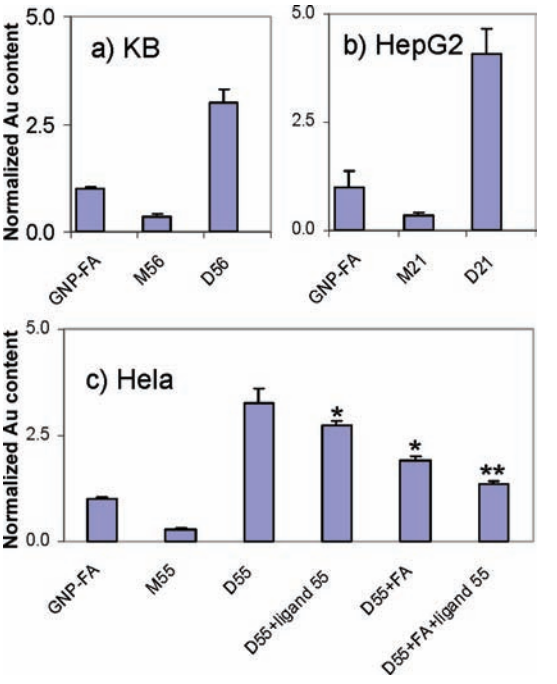

Figure 2. (a, b) Cellular uptake of selected hits and monoligand GNPs for (a) KB and (b) HepG2 cells. (c) Cellular uptake of **M55** and **D55** for Hela cells in the presence of either ligand **55** or free FA. The GNP concentration for all experiments was 50 μg/mL. The data represent means ± standard deviations of results from three experiments. The labels * and ** indicate $P < 0.05$ and $P < 0.01$, respectively, vs **D55**, as determined by Student's t test.

additive effect, suggesting a possible cooperative multivalent effect. We compared the cell binding with the computed LogD at pH 7.4 and molecular surface area, and no correlations were found, excluding the possibility that the enhancement was due to nonspecific interactions from the secondary ligands (Figure S8). To further investigate whether the specific interactions between the secondary ligands and cell surface receptors were responsible for the enhancement, we preincubated cells with free FA, ligand **55**, or both before adding **D55**. The competing free ligands effectively blocked the cell binding for Hela cells (Figure 2c), indicating that the enhanced cell recognition was likely due to the cooperative binding of both ligands to their respective receptors.

Besides the sharp differentiation of cells with an overexpressed common receptor, the DLNA was also used to differentiate cells that had high and low expressions of a common primary receptor with different surface receptor profiles around the primary receptor. This was accomplished by scanning the surfaces of Hela and A549 cells with the array. A549 cells express very low levels of FR and should have different surrounding receptors than in Hela cells because of their different organ origin. As shown above, scanning the surface of the Hela cells identified **D55** as a GNP that binds with high affinity. The binding of **GNP-FA** to Hela cells was enhanced by 100% relative to its binding to A549 cells. With dual-ligand GNP **D55,** the cell binding to Hela cells was enhanced by 400% relative to its binding to A549 cells (Figure 3a). Since cellular uptake of GNPs may promote the detrimental effects of X-ray radiation on cell viability,[23−26] we validated this enhancement by comparing the radiation-induced cell death in these two cell lines. Even at the highest dose of **D55** (150 μg/mL), X-ray irradiation (130 kV for a single dose of 10 Gy) did not induce a detectable amount of cell death in A549 cells (Figure 3b). The same dose of X-rays induced 60% cell death in FR-positive Hela cells (Figure 3b). Our data showed that X-ray radiation selectively killed cells with high levels of FRs (Hela) but did not harm cells with low levels of FRs (A549).

In summary, to mimic multivalent cell−cell recognition, we employed a dual-ligand combinatorial GNP array to scrutinize the cell surface to identify the most selective nanoparticles. Selected nanoparticles distinguish cells that have a common receptor at high or low expression levels with different surrounding receptor profiles. The sensitive differentiation of cells with high expression of a common primary receptor and different secondary receptor profiles potentially provides an opportunity to treat patients at a personalized medicine level. The enhancement of

dx.doi.org/10.1021/ja108527y | J. Am. Chem. Soc. 2011, 133, 680–682

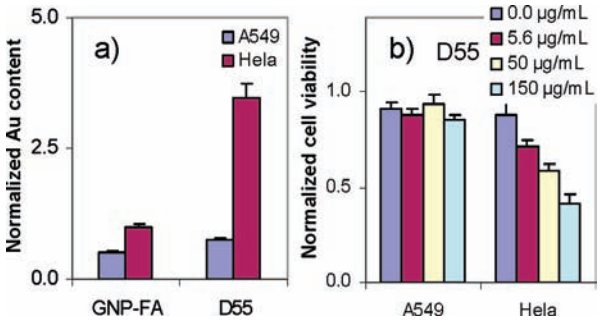

Figure 3. (a) Cellular uptake of **GNP-FA** and **D55** for A549 (nontarget) and Hela (target) cells. The GNP concentration for all experiments was 50 μg/mL. (b) Survival rate of A549 and Hela cells with various concentrations of **D55**. The X-ray experiments were performed using the Minishot X-ray cabinet at 130 kV for a single dose of 10 Gy. The data represent means ± standard deviations of the results from three experiments.

contrast between cells with high and low levels of a common primary receptor offers opportunities to target diseased cells (e.g., cancer cells) while minimizing damage to normal cells in drug delivery and radiation therapy.

■ ASSOCIATED CONTENT

Supporting Information. Experimental section; characterization of dual-ligand GNPs by UV−vis spectroscopy, TEM, DLS, ζ potential measurements, and HPLC/MS/UV/CLND; and cellular uptake of dual-ligand GNPs in Hela, KB, and HepG2 cells. This material is available free of charge via the Internet at http://pubs.acs.org.

■ AUTHOR INFORMATION

Corresponding Author
dr.bingyan@gmail.com

■ ACKNOWLEDGMENT

We thank Sharon Frase for TEM images and Thomas Mohaupt and Paul Thomas for assistance in X-ray experiments. This work was supported by the National Basic Research Program of China (973 Program, 2010CB933504), the National Natural Science Foundation of China (21077068), the National Cancer Institute (P30CA027165), the American Lebanese Syrian Associated Charities (ALSAC), and St. Jude Children's Research Hospital.

■ REFERENCES

(1) Torchilin, V. *Expert Opin. Drug Delivery* **2008,** *5,* 1003–1025.
(2) Arruebo, M.; Valladares, M.; Gonzalez-Fernandez, A. *J. Nanomater.* **2009,** No. 489389.
(3) Lee, S.; Xie, J.; Chen, X. Y. *Biochemistry* **2010,** *49,* 1364–1376.
(4) Pangburn, T. O.; Petersen, M. A.; Waybrant, B.; Adil, M. M.; Kokkoli, E. *J. Biomech. Eng.* **2009,** *131,* No. 074005.
(5) Keefe, A. D.; Pai, S.; Ellington, A. *Nat. Rev. Drug Discovery* **2010,** *9,* 537–550.
(6) Lee, J. H.; Yigit, M. V.; Mazumdar, D.; Lu, Y. *Adv. Drug Delivery Rev.* **2010,** *62,* 592–605.
(7) Ray, P.; White, R. *Pharmaceuticals* **2010,** *3,* 1761–1778.
(8) Garcia, I.; Marradi, M.; Penades, S. *Nanomedicine* **2010,** *5,* 777–792.
(9) Blondin, C.; Bataille, I.; Letourneur, D. *Crit. Rev. Ther. Drug Carrier Syst.* **2000,** *17,* 327–375.
(10) Lemarchand, C.; Gref, R.; Couvreur, P. *Eur. J. Pharm. Biopharm.* **2004,** *58,* 327–341.
(11) Weissleder, R.; Kelly, K.; Sun, E. Y.; Shtatland, T.; Josephson, L. *Nat. Biotechnol.* **2005,** *23,* 1418–1423.
(12) Choi, H. S.; Liu, W. H.; Liu, F. B.; Nasr, K.; Misra, P.; Bawendi, M. G.; Frangioni, J. V. *Nat. Nanotechnol.* **2010,** *5,* 42–47.
(13) Ross, J. F.; Chaudhuri, P. K.; Ratnam, M. *Cancer* **1994,** *73,* 2432–2443.
(14) Wu, M.; Gunning, W.; Ratnam, M. *Cancer Epidemiol., Biomarkers Prev.* **1999,** *8,* 775–782.
(15) Kluza, E.; van der Schaft, D. W. J.; Hautvast, P. A. I.; Mulder, W. J. M.; Mayo, K. H.; Griffioen, A. W.; Strijkers, G. J.; Nicolay, K. *Nano Lett.* **2010,** *10,* 52–58.
(16) Saul, J. M.; Annapragada, A. V.; Bellamkonda, R. V. *J. Controlled Release* **2006,** *114,* 277–287.
(17) Murase, Y.; Asai, T.; Katanasaka, Y.; Sugiyama, T.; Shimizu, K.; Maeda, N.; Oku, N. *Cancer Lett.* **2010,** *287,* 165–171.
(18) Ying, X.; Wen, H.; Lu, W. L.; Du, J.; Guo, J.; Tian, W.; Men, Y.; Zhang, Y.; Li, R. J.; Yang, T. Y.; Shang, D. W.; Lou, J. N.; Zhang, L. R.; Zhang, Q. *J. Controlled Release* **2010,** *141,* 183–192.
(19) Quan, C. Y.; Chang, C.; Wei, H.; Chen, C. S.; Xu, X. D.; Cheng, S. X.; Zhang, X. Z.; Zhuo, R. X. *Nanotechnology* **2009,** *20,* No. 335101.
(20) Zhou, H. Y.; Mu, Q. X.; Gao, N. N.; Liu, A. F.; Xing, Y. H.; Gao, S. L.; Zhang, Q.; Qu, G. B.; Chen, Y. Y.; Liu, G.; Zhang, B.; Yan, B. *Nano Lett.* **2008,** *8,* 859–865.
(21) Zhang, B.; Xing, Y. H.; Li, Z. W.; Zhou, H. Y.; Mu, Q. X.; Yan, B. *Nano Lett.* **2009,** *9,* 2280–2284.
(22) Zhou, H. Y.; Li, X.; Lemoff, A.; Zhang, B.; Yan, B. *Analyst* **2010,** *135,* 1210–1213.
(23) Liu, C. J.; Wang, C. H.; Chien, C. C.; Yang, T. Y.; Chen, S. T.; Leng, W. H.; Lee, C. F.; Lee, K. H.; Hwu, Y.; Lee, Y. C.; Cheng, C. L.; Yang, C. S.; Chen, Y. J.; Je, J. H.; Margaritondo, G. *Nanotechnology* **2008,** *19,* No. 295104.
(24) Liu, C. J.; Wang, C. H.; Chen, S. T.; Chen, H. H.; Leng, W. H.; Chien, C. C.; Wang, C. L.; Kempson, I. M.; Hwu, Y.; Lai, T. C.; Hsiao, M.; Yang, C. S.; Chen, Y. J.; Margaritondo, G. *Phys. Med. Biol.* **2010,** *55,* 931–945.
(25) Rahman, W. N.; Bishara, N.; Ackerly, T.; He, C. F.; Jackson, P.; Wong, C.; Davidson, R.; Geso, M. *Nanomed. Nanotechnol.* **2009,** *5,* 136–142.
(26) Kong, T.; Zeng, J.; Wang, X. P.; Yang, X. Y.; Yang, J.; McQuarrie, S.; McEwan, A.; Roa, W.; Chen, J.; Xing, J. Z. *Small* **2008,** *4,* 1537–1543.